Am. J. Trop. Med. Hyg., 88(6), 2013, pp. 1170–1179
doi:10.4269/ajtmh.12-0674

The Role of Innate versus Adaptive Immune Responses in a Mouse Model of O'Nyong-Nyong Virus Infection

Robert L. Seymour, Shannan L. Rossi, Nicholas A. Bergren, Kenneth S. Plante, and Scott C. Weaver*

Institute for Human Infections and Immunity, Center for Tropical Diseases, and Department of Pathology, University of Texas Medical Branch, Galveston, Texas

Abstract. O'nyong-nyong virus (ONNV), an alphavirus closely related to chikungunya virus (CHIKV), has caused three major epidemics in Africa since 1959. Both ONNV and CHIKV produce similar syndromes with fever, rash, and debilitating arthralgia. To determine the roles of the innate and adaptive immune responses, we infected different knockout mice with two strains of ONNV (SG650 and MP30). Wild-type, RAG1 KO, and IFNγR KO mice showed no signs of illness or viremia. The STAT1 KO and A129 mice exhibited 50–55% mortality when infected with SG650. Strain SG650 was more virulent in the STAT1 KO and A129 than MP30. Deficiency in interferon α/β signaling (A129 and STAT1 KO) leaves mice susceptible to lethal disease; whereas a deficiency of interferon γ signaling alone had no effect on survival. Our findings highlight the importance of type I interferon in protection against ONNV infection, whereas the adaptive immune system is relatively unimportant in the acute infection.

INTRODUCTION

O'nyong-nyong virus (ONNV) is a mosquito-borne virus in the family *Togaviridae,* genus *Alphavirus.* It shares 90% nucleotide sequence identity with chikungunya virus (CHIKV), which recently caused major outbreaks in the Indian Ocean, India, and Southeast Asia.[1–6] O'nyong-nyong virus has caused three major outbreaks of disease in Africa.[7–10] The first occurred in Uganda in the late 1950s and early 1960s and affected over 2 million people.[7] The last two outbreaks occurred in 1996 and 2003, affecting tens of thousands of people.[8–11] O'nyong-nyong virus causes a similar syndrome to CHIKV, Ross River virus (RRV), and other Old World arthritic alphaviruses, characterized by fever, rash, debilitating arthralgia, and myalgia.[7–11] The disease is self-limiting and lasts a few days, though some patients have more persistent arthrlagia.[12] In contrast to CHIKV, which has recently been shown to produce neurologic manifestations and death in some individuals, ONNV is not known to cause fatal disease.[6] The true incidence of ONNV infection is not known, because the syndrome it causes is very similar to that caused by CHIKV, dengue virus, and other African tropical infectious diseases that are almost clinically indistinguishable. This probably leads to frequent underreporting of ONNV infections. Furthermore, it is difficult to distinguish antibodies generated in response to ONNV versus CHIKV infection because of nearly complete cross-reactivity.[9,13] This difficulty with serodiagnosis is particularly important because control measures differ for ONNV and CHIKV as a result of the different genera of mosquitoes that serve as vectors.

Although CHIKV and ONNV produce similar clinical syndromes, their transmission cycles and geographic distributions differ markedly. Chikungunya virus has repeatedly emerged from enzootic cycles in Africa to initiate urban human-mosquito-human cycles in Africa, Asia, and even Europe, whereas ONNV has never been detected outside of sub-Saharan Africa.[14,15] Unlike most other alphaviruses that are transmitted by *Aedes* spp. and *Culex* spp. mosquitoes, ONNV is the only known alphavirus transmitted by *Anopheles* mosquitoes (principally *Anopheles gambiae* and *Anopheles funestus*).[16,17] In addition, although the reservoir host for many alphaviruses is known (typically non-human primates, birds, or rodents), a reservoir host for ONNV has not been incriminated. Humans likely serve as amplification hosts during epidemics, but are unlikely to sustain transmission during interepidemic periods of up to decades.

The course of infection and pathogenesis of ONNV has not been well described. The generation of a convenient animal model is therefore important for understanding pathogenesis as well as for testing new therapeutics. Finally, because it is possible for ONNV to reemerge again in Africa with an unknown potential to spread to other continents, thanks to increased commerce and air travel, the development of an animal model could be critical for public health.

MATERIALS AND METHODS

Viruses. The available strains of ONNV, MP30 and SG650, were provided by Robert Tesh from the World Reference Center for Emerging Viruses and Arboviruses at the University of Texas Medical Branch (UTMB) in Galveston, TX. Strain MP30 (Gulu strain) was isolated from human serum during the first documented ONNV epidemic in late 1959. It was previously passaged 13 times in infant mouse brains and twice on Vero African green monkey kidney cell cultures. Strain SG650 was isolated from human serum during the 1996 outbreak in Uganda and has been passaged three times in Vero cells.

Cell cultures. Vero cells were obtained from the American Type Cell Culture (Bethesda, MD) and propagated at 37°C in 5% CO_2 in Dulbecco's minimum essential media (DMEM) supplemented with 10% fetal bovine serum, and 1% penicillin and streptomycin.

Animal studies. All mice were maintained in an ABSL-2 facility and experiments were done according to an approved protocol from the UTMB Institutional Animal Care and Use Committee, following the guidelines of the Association for Assessment and Accreditation of Laboratory Animal Care, International (AAALAC) and the National Institutes of Health (NIH).

The C57BL/6J, recombinase activation gene 1 knockout (RAG1 KO), and type II interferon receptor knockout (IFNγR KO) mice were purchased from Jackson Laboratories

* Address correspondence to Scott C. Weaver, Department of Pathology, University of Texas Medical Branch, Galveston, TX 77555-0610. E-mail: sweaver@utmb.edu

(Bar Harbor, ME). The RAG1 KO, and IFNγR KO mice are both on the C57BL/6J background. Signal transducer and activator of transcription 1 knockout (STAT1 KO) and 129S6 mice were purchased from Taconic Farms (Hudson, NY). The A129 (IFNα/βR KO) mice were obtained from Slobodan Paessler (UTMB). The STAT1 KO and A129 mice are on the 129S6 background.

Mice were inoculated subcutaneously (s.c.) in the back with 100 μL of ONNV at doses of 10^2 to 10^4 plaque-forming units (pfu) or were inoculated in the left rear footpad (f.p.) with 10 μL of ONNV at a dose of 10^3 pfu. Mice were weighed and monitored daily for clinical signs of illness for at least 14 days. The thickness of the f.p. was measured with a digital caliper to determine swelling. Blood obtained from the retro-orbital sinus of selected mice was clarified by centrifugation (2,500 × *g* for 5 min) and serum stored at −80°C until plaque assayed. Moribund mice were euthanized with CO_2 and tissues were either fixed for histology (see below) or weighed and stored at −80°C for measurement of viral load. In some studies, mice sacrificed on days 3 and 6 were perfused with phosphate buffered saline (PBS) before tissue collection. The PBS was injected into the left ventricle and allowed to circulate through the animal, and was drained from an incision in the right atrium. Animals were perfused with at least 50 mL of PBS until all blood was removed, indicated by clear fluid flowing from the right atrium.

Plaque assays for viremia and tissue viral load. Frozen tissues were thawed in a 10X (V/W) volume of DMEM and homogenized using a TissueLyserII (Qiagen, Valenica, CA) at 25 cycles/second for 5 minutes. The homogenate was clarified by centrifugation (2,500 × *g* for 5 min) and supernatant was removed and stored at −80°C. Plaque assays were performed on Vero cells in either 6- or 12-well plates as described previously.[18] Titrations were overlaid with 0.4% agarose in DMEM. Two or 3 days later, plates were fixed with 10% formaldehyde for at least 30 minutes and stained with crystal violet to visualize plaques.

Histology. Tissues were fixed in 10% neutral buffered formalin (RICCA Chemical Company, Arlington, TX), and bone tissue was decalcified overnight using Fixative/Decalcifier (VWR International, Radnor, PA). Organs were embedded in paraffin wax and 5 μm sections were cut for histopathological analysis. Sections for hematoxylin and eosin (H&E) staining were prepared as previously described.[19,20]

Statistics. Differences in animal weights were analyzed using two-way analysis of variance with a Tukey-Kramer post-hoc test. Significance was determined by a P value of < 0.05.

RESULTS

An intact interferon α/β response is sufficient for protection against acute ONN disease. To determine if immunocompetent mice are susceptible to ONNV infection, C57BL/6J mice were infected with 10^3 pfu, a dose that approximates the maximum amount of alphaviruses transmitted by mosquito vectors, of the SG650 strain.[21] All C57BL/6J mice survived infection (Figure 1). These mice did not develop signs of illness, nor did they develop detectable viremia within the first 6 days of infection (limit of detection 100 pfu/mL; data not shown).

To determine which portions of the immune response were necessary for protection against acute disease following ONNV infection; mice with various immunologic deficiencies were inoculated with two different strains of ONNV (SG650 and MP30). Immunodeficient mice were chosen to reflect deficiencies in the adaptive (RAG1 KO, deficient in T and B cells) and innate immune systems (A129, deficient in the IFN α/β receptor; IFNγR KO, which is deficient in interferon γ receptors, and the STAT1 KO, which is deficient in all interferon signaling). The STAT1 KO and A129 mice developed fatal disease following ONNV infection (strain SG650, 10^3 pfu) with mortality rates of about 50% (Figure 1). By day 5 post inoculation, STAT 1 KO and A129 mice began to lose weight (Figure 2A and B), which coincided with clinical signs of disease including ruffled fur, lethargy, and hunched posture. Disease worsened in the STAT 1 KO animals, with 2 of 22 mice displaying hind limb paralysis by day 8. No A129 mice exhibited limb paralysis. The RAG1 KO, IFNγR KO, C57BL/6J, and wt 129S6 mice all survived (Figure 1), appeared healthy, and maintained stable weight throughout the study (data not shown).

To test for variation in ONNV strain virulence, the same mouse strains were inoculated with 10^3 pfu of ONNV strain MP30. Again, RAG1 KO, IFNγR KO, C57BL/6J, and 129S6

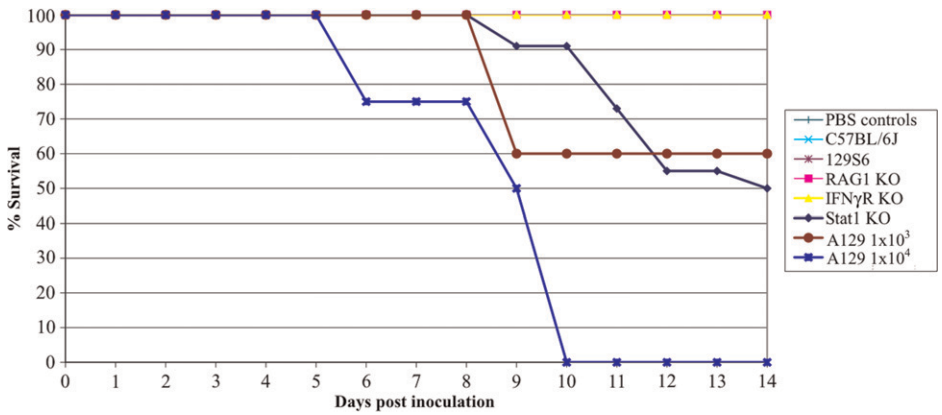

FIGURE 1. Survival of O'nyong-nyong virus (ONNV)-infected mice. Survival data are shown following subcutaneous infection of 6-week-old mice with 10^3 plaque-forming units (pfu) of ONNV (strain SG650) or 10^4 pfu where noted for A129 mice. For RAG KO-, IFNγR KO-, 129S6-, and C57BL/6J-infected mice, $N = 8$. For phosphate buffered saline (PBS)-inoculated controls, $N = 4$. For A129 infections at a dose of 10^3 pfu, $N = 5$, A129 at 10^4 pfu, $N = 4$, and PBS control, $N = 4$. For infected STAT1 KO mice, $N = 22$ and PBS control $N = 10$.

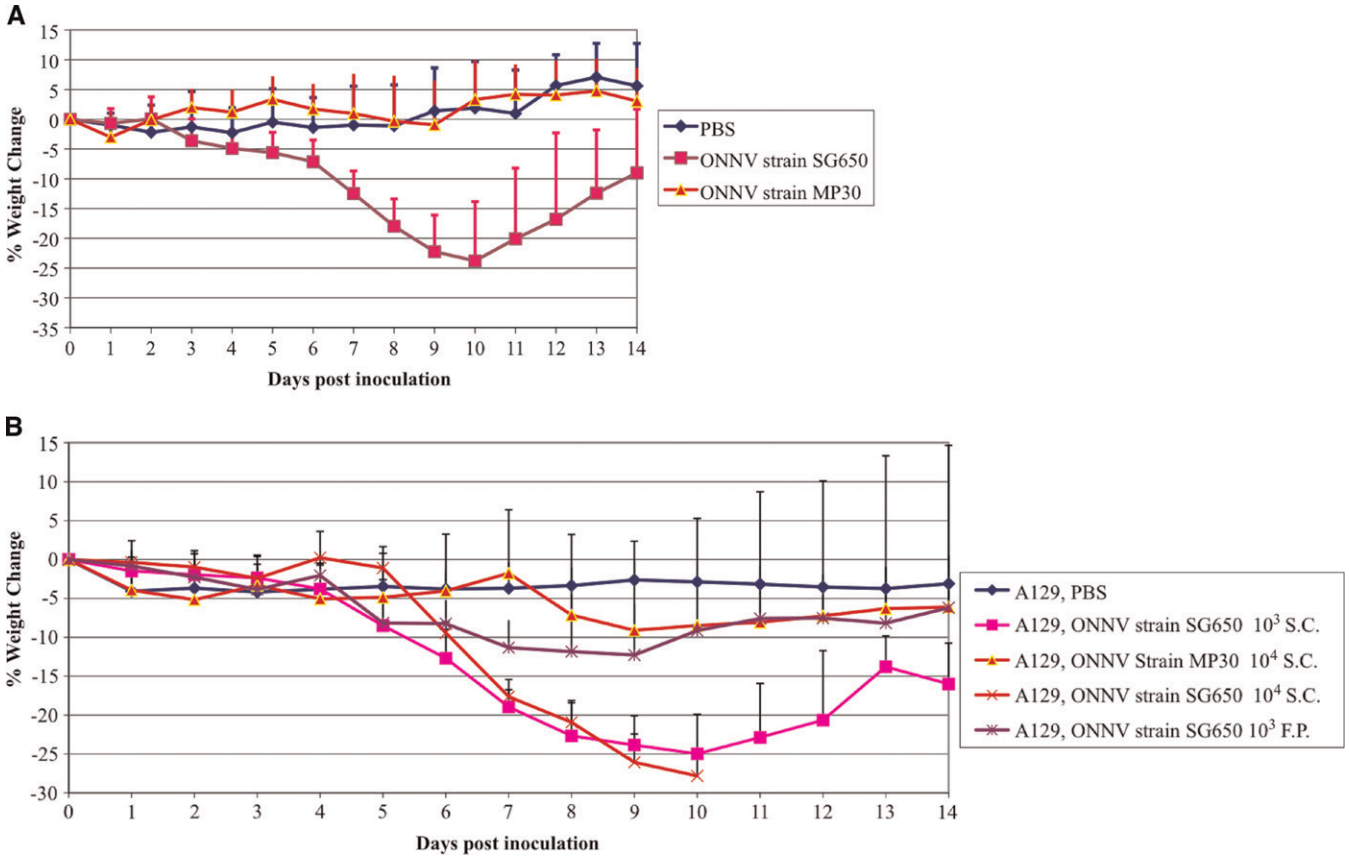

FIGURE 2. (**A**) Weight change following O'nyong-nyong virus (ONNV) infection of STAT1 KO mice. Data are shown following subcutaneous (s.c.) infection of 6-week-old mice with 10^3 plaque-forming units (pfu) of ONNV (strain SG650 or MP30). For MP30-infected mice $N = 14$; SG650 infected mice, $N = 22$, and phosphate buffered saline (PBS) controls, $N = 10$. (**B**) Weight change following ONNV infection of A129 mice. Data are shown following s.c.-infection of 6-week-old mice with 10^3 or 10^4 pfu of ONNV strain SG650, footpad (f.p.) infection of 6–8 week-old-mice with 10^3 of SG650 or s.c.-infection with 10^4 pfu of strain MP30. For MP30 infected mice, $N = 8$; SG650 s.c. 10^3 infected mice, $N = 9$; SG650 10^4 s.c. infected mice, N = 4; SG650 10^3 f.p. infected, N = 12; PBS controls, $N = 7$. Bars represent one standard deviation.

mice all survived for the duration of the study and showed no clinical signs of disease (data not shown). Unlike ONNV strain SG650 infections, STAT1 KO mice all survived infection with the MP30 strain (data not shown). Some mice showed morbidity with mild weight loss (Figure 2A), hunched posture, lethargy, and ruffled fur beginning at day 8, but all mice began to recover by day 10. Because only a minority of mice lost weight, there was no statistical difference between the mean weights of the sham (PBS) and MP30-infected groups. A129 mice were also inoculated with 10^3 pfu of ONNV strain MP30. These mice appeared healthy throughout the study (data not shown).

To test for virulence at a higher dose, A129 mice were infected with 10^4 pfu of MP30. Only 3 of 8 mice showed clinical signs of illness. There was a loss in mean weight, which was seen beginning at days 8–9 (Figure 2B). One mouse developed hind limb paralysis at day 9. This mouse only developed weight loss concurrent with limb paralysis and never displayed ruffled fur. Recovery of hind limb function began on day 12 and continued until it was euthanized on day 22 post inoculation caused by increased weight loss. A second A129 mouse had ruffled fur, weight loss, and hind limb weakness, which later resolved. Despite a stabilized weight between days 11 and 19 post inoculation this mouse was ultimately euthanized on day 22 post inoculation when weight began to drop again. A third A129 mouse developed hind limb paralysis on day 11 and was euthanized on day 14.

Because mice infected with 10^4 pfu of MP30 showed some morbidity, we infected four A129 mice with 10^4 pfu of strain SG650 to obtain a direct comparison of the two strains. All mice developed ruffled fur, lethargy, hunched posture, and weight loss beginning on day 4 (Figure 2B). The first animal died on day 6 and all expired or were euthanized by day 10 (Figure 1).

The virulence of MP30 was lower than that of SG650 in the STAT1 KO mice, as measured by weight loss and lethality. There also was a difference in weight loss between A129 mice inoculated with strains MP30 (10^4 pfu) and SG650 (10^3 pfu) on days 11–14. However, on earlier days there was no statistical difference between these groups, or between MP30 at a dose of 10^4 and PBS controls. These results in A129 mice can be explained because the 3 mice out of 8 that showed illness were severely ill, whereas the other five mice were not ill and gained weight, thus causing large standard deviations. In addition, as noted previously SG650 was 100% lethal in A129 mice at 10^4 pfu, whereas MP30 showed morbidity and mortality in 3 of 8 mice at the same dose.

To determine if the route of ONNV infection affects disease, we inoculated the footpads of A129 mice with 10^3 pfu of

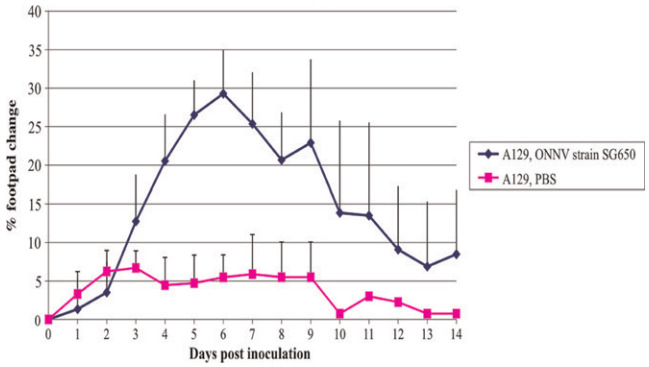

FIGURE 3. Footpad swelling in A129 mice. Data are shown following footpad infection of 6–8 week-old mice with 10^3 plaque-forming units (pfu) of ONNV (SG650, $N = 12$; PBS, $N = 5$). Error bars represent one standard deviation.

SG650. These mice exhibited f.p. swelling (Figure 3), systemic signs of illness, and weight loss (Figure 2B). Swelling was noted in those animals inoculated with ONNV by the f.p. beginning on day 3 (Figure 3). Animals inoculated in the back by the s.c. route did not exhibit f.p. swelling (data not shown). None of the animals succumbed to illness (data not shown) and no animals displayed neurologic involvement. The MP30 strain was not used in these studies because of its attenuated phenotype when delivered subcutaneously.

Viremia and tissue viral load in STAT1 KO and A129 mice. Viremia in s.c-inoculated SG650 STAT1 KO mice peaked at day 2 post infection and slowly declined to undetectable levels by day 5 (Figure 4). The SG650 s.c.-inoculated A129 mice at the same dose (10^3 pfu) exhibited a similar pattern to the STAT1 KO mice. However, the viremia was 10- to 100-fold higher at each time point tested except on day 5 (Figure 4). A 10-fold increase in the SG650 dose in A129 mice did not significantly alter peak viremia titers, but extended viremia for an extra day (Figure 4). The A129 mice inoculated in the f.p. with 10^3 pfu of SG650 had a higher titer on day 1 post infection, peaking at day 2, but progressively declined with daily titers lower than s.c.-inoculated mice until reaching undetectable levels at day 5 (Figure 4). Mice inoculated s.c. with the MP30 strain had barely detectable levels of virus in their blood. The average peak viremia of about 200 pfu/mL was reached 2 days after s.c. infection of STAT1 KO mice, although some animals had no detectable viremia (Figure 4). A peak viremia of about 500 pfu/mL was reached on day 3 in A129 mice given a s.c. dose of 10^3 pfu of MP30, comparable to that seen in similarly tested STAT1 KO mice. There was no detectable viremia in A129 mice given 10^4 pfu of strain MP30 by the s.c. route (data not shown). No other strains of type I interferon competent mice tested (RAG1 KO, IFNγR KO, 129S6 or C57BL/6J) exhibited viremia from either SG650 or MP30 s.c. infections (data not shown).

To begin to characterize the pathogenesis of ONNV infection, A129 mice were injected (either s.c. or f.p.) with 10^3 pfu of the SG650 strain. Tissues were harvested following perfusion on days 3 and 6 post inoculation. Mice euthanized on day 9 were not perfused. Virus detection in tissues by plaque assays from days 3 and 6 is summarized in Table 1. The route of inoculation did not appear to have a drastic effect on the location or load of virus within the mice. Generally, organ titers were higher on day 3 than day 6 post inoculation. Additionally, fewer organs contained detectable virus as time post infection increased (Table 1); no virus was detected from any organ on day 9 (data not shown).

Interestingly, skeletal muscle from the left leg, which was the site of f.p. injection in some mice, contained 3.6–5.9 logs of ONNV on days 3 and 6 post infection, regardless of the route (f.p. or s.c.) and location of inoculation (f.p. or back) (Table 1). The right leg was not tested in mice inoculated by the s.c. route. Muscle on the contralateral side of f.p. inoculation was also positive in some mice, suggesting that ONNV is capable of spreading and infecting skeletal muscle far removed from the site of initial infection.

We next sought to determine the viral loads present in animals that succumbed to illness. The A129 and STAT1 KO mice were infected with 10^3 pfu of SG650, and organs were

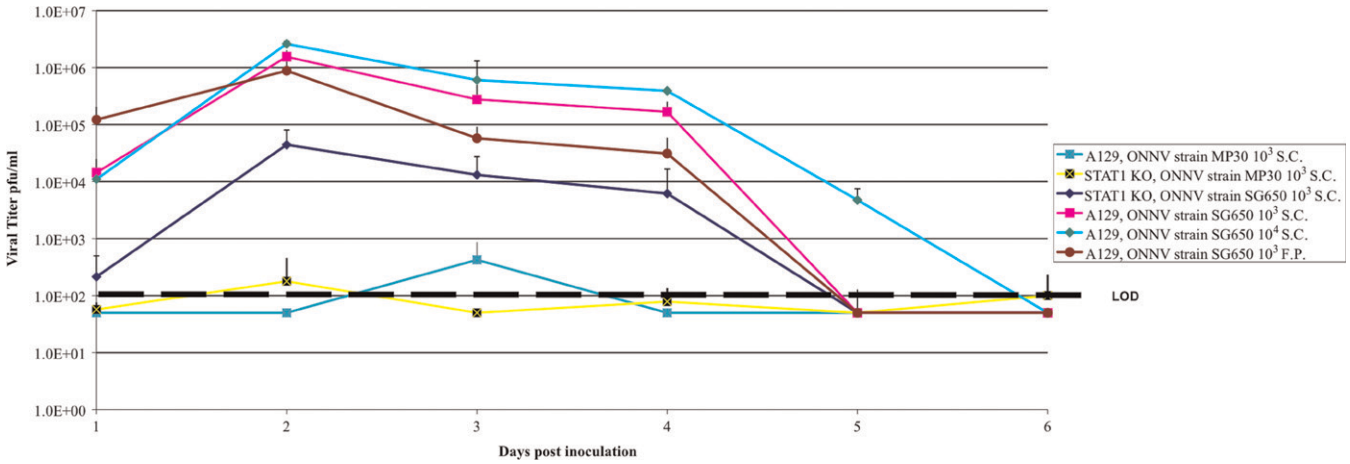

FIGURE 4. Viremia in STAT1 and A129 mice. Data are shown following subcutaneous or footpad infection of 6–8 week-old mice with 10^3 or 10^4 plaque-forming units (pfu) of O'nyong-nyong virus (ONNV). For STAT1 KO mice infected subcutaneously (s.c.) with SG650 and MP30, $N = 7$; A129 mice infected s.c. with SG650 10^3 pfu, $N = 5$; A129 mice infected s.c with SG650 10^4 pfu, $N = 4$; A129 mice infected s.c. with 10^3 pfu of MP30, $N = 5$; A129 mice infected via footpad (f.p.) with 10^3 pfu of SG650; $N = 5$. The limit of detection of the plaque assay was 100 pfu/mL. Negative animals were assigned a value of one-half the limit of detection. Error bars represent one standard deviation.

TABLE 1
Viral loads in organs of A129 mice days 3 and 6 post inoculation

Organs	Fraction of animals positive for ONNV 3 days after f.p. inoculation	Viral load* (Log_{10} pfu/g)	Fraction of animals positive for ONNV 6 days after f.p. inoculation	Viral load* (Log_{10} pfu/g)	Fraction of animals positive for ONNV 3 days after s.c. inoculation	Viral load* (Log_{10} pfu/g)	Fraction of animals positive for ONNV 6 days after s.c. inoculation	Viral load* (Log_{10} pfu/g)
Brain	0/3	< 2.0	1/3	4.9	0/3	< 2.0	2/3	3.7–4.8
Heart	1/3	2.0	0/3	< 2.0	1/3	3.0	1/3	3.7
Lung	2/3	3.6–3.9	2/3	3.4–3.6	2/3	3.8	1/3	2.8
Liver	2/3	3.9–4.3	0/3	< 2.0	1/3	4.3	0/3	< 2.0
Spleen	3/3	3.6–4.3	0/3	< 2.0	2/3	3.3–4.0	0/3	< 2.0
Kidney	0/3	< 2.0	0/3	< 2.0	1/3	3.7	0/3	< 2.0
Right leg	1/3	3.4	2/3	4.2–4.6	ND	ND	ND	ND
Left leg†	3/3	5.4–5.9	3/3	4.7	3/3	3.6–4.8	3/3	4.0–5.6

*Limit of detection = 2 log_{10} pfu/gram.
†Side of inoculated footpad.
ONNV = O'nyong-nyong virus; f.p. = footpad; pfu = plaque-forming units; s.c. = subcutaneously; ND = not determined.

harvested when mice were moribund. Virus was undetectable (< 100 pfu/gram) from moribund A129 mice (harvested days 9–12). This observation is consistent with the lack of detectable virus found on the day 9 harvests of non-moribund mice. Moribund STAT1 KO mice, however, contained virus within the brain, heart, and skeletal muscle (Table 2). These animals were sacrificed between days 9 and 12 post inoculation. Virus found in these organs represented the true viral organ load because these mice were not viremic. Moribund A129 mice, which were inoculated with 10^4 pfu of strain MP30, had no detectable virus in any organ (data not shown).

Lethality of ONNV is dependent on mouse age. To determine if the outcome of ONNV infection is also age-dependent like that of other alpahviruses, we used 12–16-week-old STAT1 KO mice and inoculated them s.c. with varying does of ONNV strain SG650. STAT1 KO mice were chosen for these studies due to the more severe histologic changes (see next section) and more severe clinical course than in the A129, though lethality was similar in the two mouse strains. These older mice exhibited severe morbidity and weight loss beginning on day 4 (Figure 5) for all doses. In contrast to the 50% mortality seen in 6-week-old mice after a dose of 10^3 pfu (Figure 1), all 12–16-week-old mice began to recover by day 9 or 10 post inoculation and survived regardless of the infectious dose.

Murine ONNV infection produces a marked mixed inflammatory infiltrate with numerous monocytes. Next, we sought to characterize the pathologic changes in moribund STAT1 KO mice induced by s.c. ONNV infection with 10^3 pfu of strain SG650. Histopathologic and gross evaluation of the brain, heart, lung, liver, spleen, kidney, bowel, skeletal muscle, and joint were performed (Figure 6). There was a marked mixed inflammatory infiltrate with numerous monocytes in all organs examined. No gross lesions were identified in these tissues. The below histologic changes were identified in the vast majority of mice with only a difference in the degree of inflammation and tissue damage.

TABLE 2
Viral load in moribund STAT1 KO mice

Organs*	Fraction of animals positive for ONNV	Time of death (dpi)	Viral load† (Log_{10} pfu/g)
Brain	4/11	9–10	4.2–5.8
Heart	4/11	9–12	2.9–5.3
Lung	0/11	N/A	NA
Liver	0/11	N/A	NA
Spleen	0/11	N/A	NA
Kidney	0/11	N/A	NA
Skeletal muscle	5/11	9–12	3.0–5.6

*6-week-old mice infected with 10^3 pfu of SG650.
†Limit of detection = 2 log_{10} pfu/gram.
ONNV = O'nyong-nyong virus; pfu = plaque-forming units.

The brain (Figure 6A) exhibited meningoencephalitis, with the severity of the inflammation increasing in animals that survived longer. The inflammation was characterized by perivascular cuffing, neuronal death, and a mixed inflammatory infiltrate with numerous monocytes, with horseshoe-shaped nuclei and abundant eosinophilic cytoplasm. Although the infiltrate was predominantly monocytic, numerous neutrophils and lymphocytes were also present. The heart (Figure 6B) exhibited myocarditis as indicated by an inflammatory infiltrate composed predominantly of monocytes with scattered neutrophils and lymphocytes. Numerous cardiac myocytes had a wavy appearance upon H&E staining, consistent with loss of viability. Inflammation in the lung (Figure 6C) was again predominantly composed of monocytes with scattered neutrophils and lymphocytes. Bronchial epithelium showed reactive changes; the alveolar septae were distended with the previously mentioned inflammatory infiltrate, and there was reduction in alveolar space possibly caused by enlargement of the septae and alveolar collapse. The skeletal muscle of the leg (Figure 6D) exhibited the same mixed inflammatory infiltrate as seen in other organs. Monocytes, lymphocytes, and scattered neutrophils surrounded dead and dying skeletal myocytes. The ankle joint (Figure 6E) showed thickening of the synovial lining, edema, and a mixed inflammatory infiltrate. The architecture of the liver (Figure 6F) was maintained, and no damage to the bile ducts or vascular structures was noted. However, scattered throughout the hepatic lobules were collections on inflammatory cells, mainly monocytes in microgranulomas. The kidney (Figure 6G) parenchyma retained its normal architecture, and glomeruli showed mild increased cellularity. The interstitium had several collections of inflammatory cells composed predominantly of monocytes with occasional neutrophils and lymphocytes. There was no necrosis evident in the glomeruli and tubules. The spleen (Figure 6H) exhibited an intact architecture with appropriate placement and numbers of lymphoid follicles. However, the spleens of ONNV-infected mice differed in one important way from controls: the red pulp of infected mice exhibited an infiltrate of predominantly monocytoid cells with abundant eosinophilic cytoplasm and numerous reactive lymphoblasts. Necrosis was not noted in the spleen. Sections of the bowel (Figure 6I) showed the same monocytic inflammatory infiltrate seen in the other organs. The bowel wall was thickened and the inflammatory infiltrate was present in all layers, from

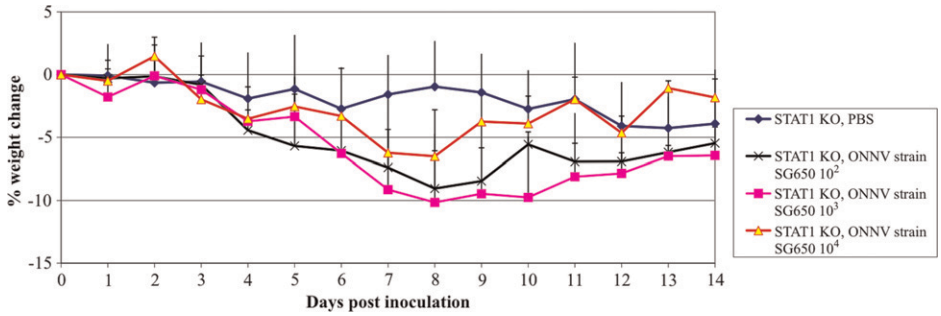

FIGURE 5. Weight change following O'nyong-nyong virus (ONNV) infection of 12–16-week-old STAT1 KO mice. Data are shown following subcutaneous infection of 12–16-week-old mice with 10^2, 10^3, or 10^4 plaque-forming units (pfu) of ONNV (strain SG650). For the 10^2 and 10^4 cohorts, $N = 3$; for the 10^3 group, $N = 11$; and for the phosphate buffered saline (PBS) control group, $N = 6$. Error bars represent one standard deviation.

the luminal glands to the serosa. There was no overt necrosis of intestinal glands. Although no overt destruction of cells was seen in the spleen, kidney, and bowel, this does not imply that the inflammation did not functionally compromise these organs.

Histologic and gross examination was also carried out on A129 mice inoculated with 10^3 pfu of SG650 either s.c. or by f.p. and subsequently sacrificed on days 3, 6, and 9. These animals had noticeably enlarged spleens with large reactive follicles and replacement of the red pulp by immunoblasts and other inflammatory cells starting on day 3 and beginning to resolve on day 9 (Figure 7A–I). This splenomegaly and large numbers of reactive follicles are the hallmarks of a

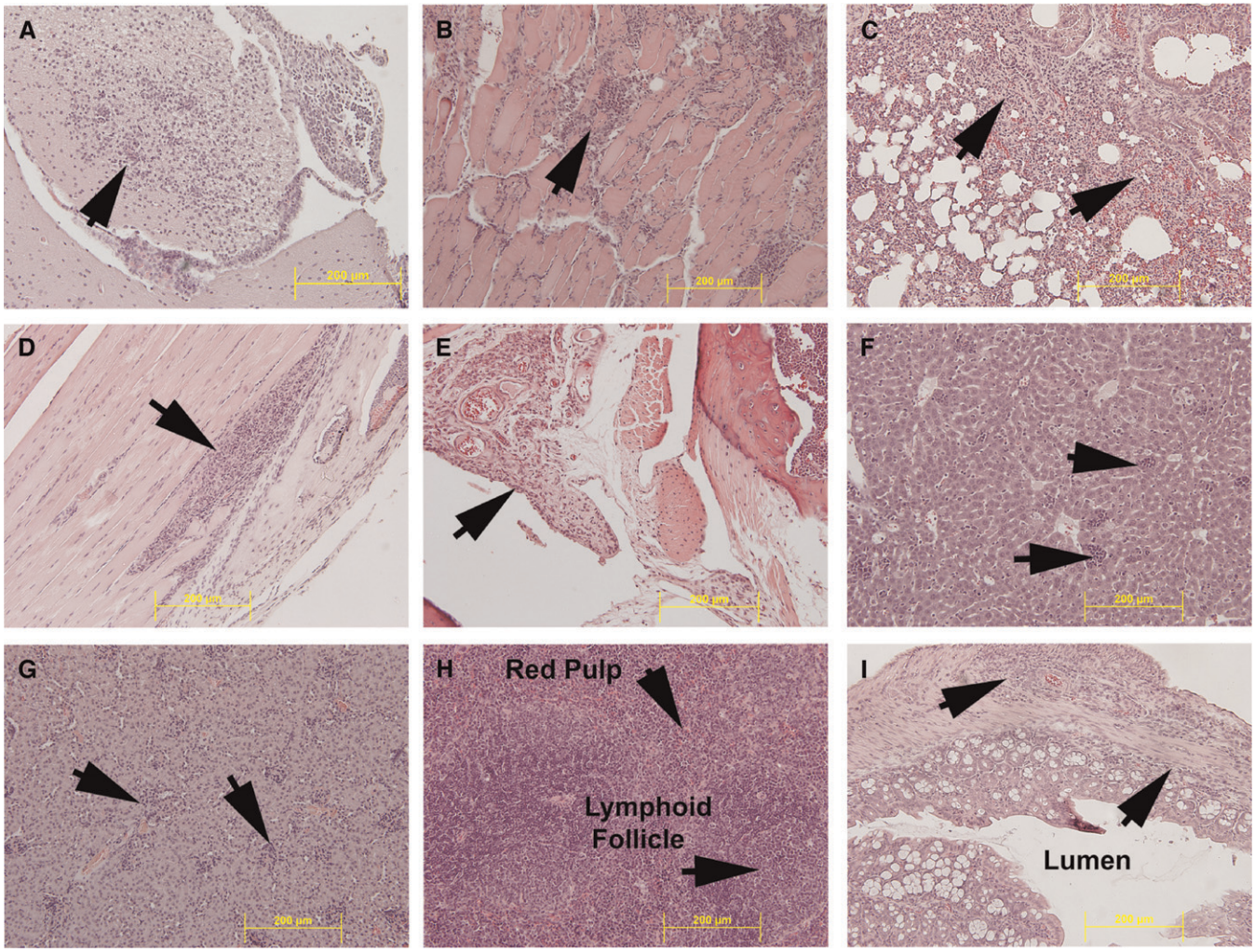

FIGURE 6. Histopathologic analysis of organs in STAT1 KO mice. Hematoxylin and eosin (H&E) stained sections of organs are shown: (**A**) brain, (**B**) heart, (**C**) lung, (**D**) skeletal muscle, (**E**) joint space, (**F**) liver, (**G**) kidney, (**H**) spleen, (**I**) bowel. All images are at 20× magnification. The yellow bar shows 200 μM scale. Arrows indicate inflammation except where noted.

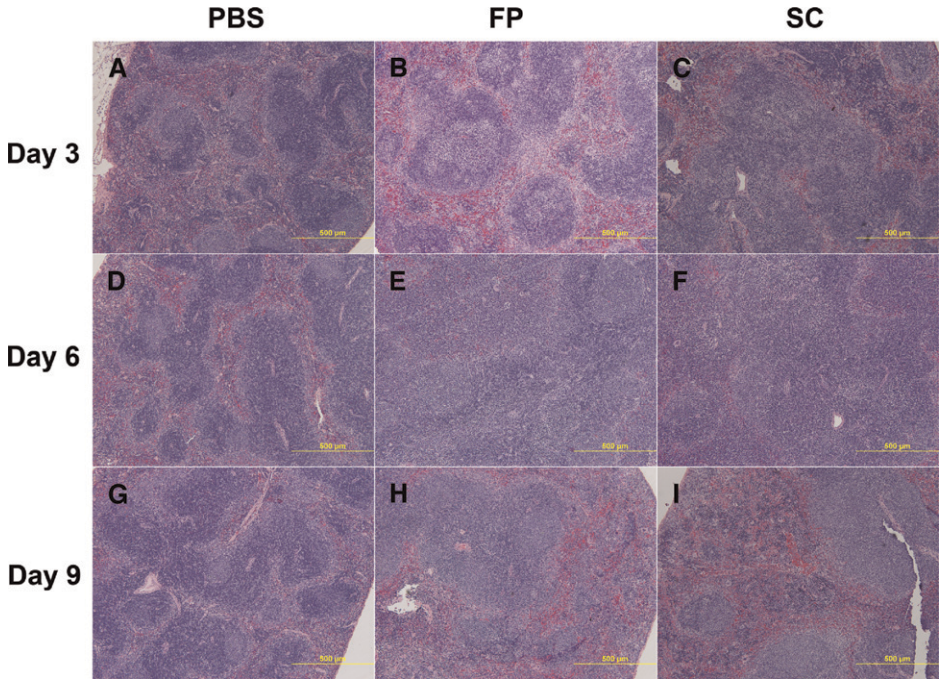

FIGURE 7. Histopathologic analysis of spleen in A129 mice. Hematoxylin and eosin (H&E) stained sections are shown: (**A**) phosphate buffered saline (PBS) day 3, (**B**) footpad (f.p.)-inoculated day 3, (**C**) subcutaneously (s.c.)-inoculated day 3, (**D**) PBS day 6, (**E**) f.p.-inoculated day 6, (**F**) s.c.-inoculated day 6, (**G**) PBS day 9, (**H**) f.p.-inoculated day 9, (**I**) s.c.-inoculated day 9.

reactive spleen. The livers exhibited microgranulomas from day 3 through 9, which were consistent with the findings for the STAT1 KO mice (Figure 6F). Skeletal muscle of both the s.c.- and f.p.-inoculated mice showed no detectible histopathologic change on day 3 (Figure 8A–C). By day 6 post inoculation, both groups began to show a slight mixed inflammatory infiltrate in the adipose tissue of the leg, with some infiltrate of the muscle tissue (Figure 8D–F). By day 9 post inoculation, both groups displayed severe myositis and tenosynovitis in both legs (Figure 8G–I). The brain, lung, heart, bone, bowel, stomach, and kidney showed no significant histopathologic change.

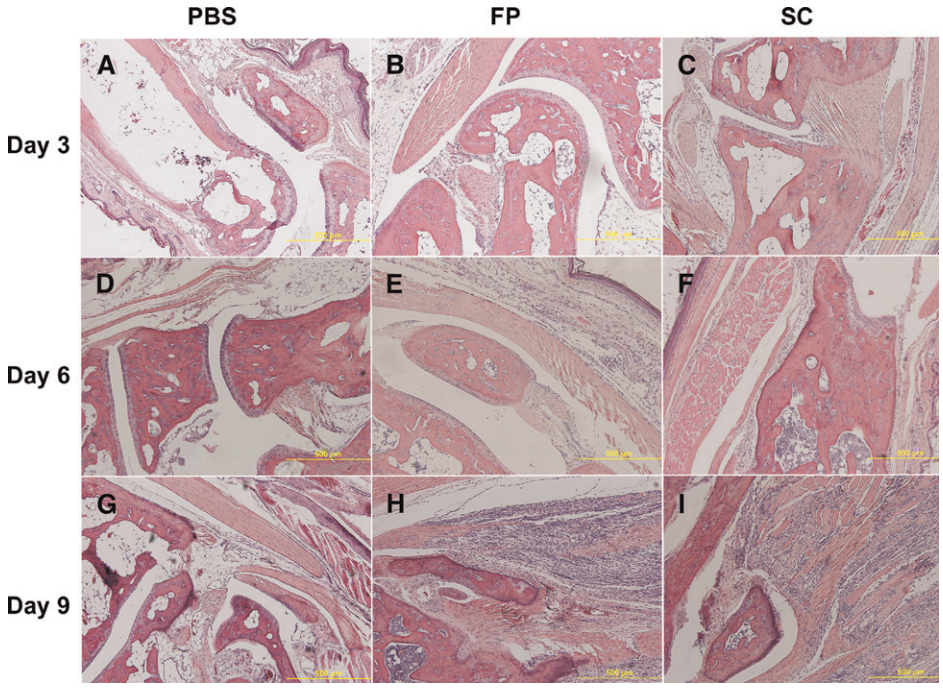

FIGURE 8. Histopathologic analysis of skeletal muscle in A129 mice. Hematoxylin and eosin (H&E) stained sections are shown: (**A**) phosphate buffered saline (PBS) day 3, (**B**) footpad (f.p.)-inoculated day 3, (**C**) subcutaneously (s.c.)-inoculated day 3, (**D**) PBS day 6, (**E**) f.p.-inoculated day 6, (**F**) s.c. inoculated day 6, (**G**) PBS day 9, (**H**) f.p.-inoculated day 9, (**I**) s.c.-inoculated day 9.

DISCUSSION

Similar to other Old World alphaviruses like CHIKV and RRV, ONNV causes a clinical syndrome characterized by fever, rash, debilitating arthralgia, and myalgia. Many studies have been done into the pathogenesis of CHIKV and RRV, including those of human patients, the development of animal models, and in the case of CHIKV, non-human primate models. These studies have shown a critical role for macrophages/monocytes in the pathogenesis of these viruses.[22–24] In addition, these studies have shown the importance of type I interferons and complement in mice.[25–29] In humans, overlap has been identified between persistent CHIKV and rheumatoid arthritis; and proinflammatory mediators seem to play a role in disease progression and persistence.[30–33] However, the study of ONNV has received relatively little attention since its discovery, though it was the cause of one of the largest known arboviral outbreaks in the late 1950s and early 1960s in Uganda. Other than its clinical symptoms, very little is known about the pathogenesis of ONNV virus compared with CHIKV and RRV.

This study has begun to elucidate the portions of the murine immune response involved in protection against acute disease following ONNV infection. Our survival results showed three major points: 1) the innate immune response is sufficient to control ONNV infection after a dose of 10^3 pfu, as indicated by the lack of detectable viremia and/or clinical illness in RAG1 KO mice. It is possible that higher doses of ONNV given to RAG1 KO might generate transient viremia and clinical signs of illness. However, we chose a dose of 10^3 pfu to approximate the amount of alphaviruses transmitted by mosquito vectors.[21] These results do not imply that the adaptive immune response, which confers memory and protection from future challenges of ONNV, is unimportant. Rather, the adaptive immune response does not appear to be essential for survival during acute infection; 2) IFNγ by itself is not necessary to control acute disease. The IFN-γR KO mice did not generate detectable viremia or signs of illness; 3) The IFN α/β response appears to be very important for protection against acute disease. The A129 mice, which are deficient for IFN α/β receptors, and STAT 1 KO mice, which are deficient in IFN α/β and γ signaling, exhibited 50–55% mortality after a s.c dose of 10^3 pfu. These findings are similar to other studies showing the importance of the IFN α/β response has in host defense against other alphavirus infections.[28,29,34–37]

Our data are consistent with the findings of others that have demonstrated lethality from ONNV in the AG129 mouse, which is deficient in type I and type II interferon receptors; and with those of the closely related alphavirus, CHIKV.[38,39] Mice deficient in STAT1 and in type I interferon receptors show the same mortality when inoculated s.c., although histologically and clinically STAT1 KO mice show more severe disease. These findings imply that, although IFNγ is not necessary on its own in protection against infection, it might compensate for a type I interferon deficiency to some extent. The finding of mortality in s.c.-inoculated A129 mice is in contrast to those inoculated by the f.p. Although these animals did show clinical signs of illness, none died at the same dose, which caused 50% mortality in the s.c.-inoculated mice.

It has been shown that mouse f.p. inoculation with CHIKV, although not totally recapitulating human disease, does result in severe myositis and tenosynovitis in the inoculated leg.[40–42] In this study, we showed very similar results to those seen with CHIKV-induced f.p. swelling and severe myositis.[40–42] There is a mixed inflammatory infiltrate composed predominately of monocytic and some lymphoid cells. In addition to these findings, we have shown myositis occurs in both hind limbs regardless of the site of inoculation.

It is not surprising that we found infectious ONNV in the brain and skeletal muscle of A129 mice. The presence of virus in the heart could be a function of myocyte tropism as has been reported in CHIKV infection.[43,44] It is of interest that the inflammatory infiltrate seen in the tissues of all animal groups is composed predominantly of monocytes. In the STAT1 KO mice, cell death was seen in the brain, heart, skeletal muscle, and to an extent in the liver. Other tissues, although they exhibited an inflammatory infiltrate, did not appear to have a high level of overt cellular death. However, this does not imply the absence of organ dysfunction. The infiltrate did not have a high number of lymphocytes. In A129 mice the inflammatory infiltrates were observed only in the skeletal muscle and liver. The infiltrate in the liver was composed of microgranulomas. These changes were seen independent of the route of inoculation. The changes noted in the spleen most likely represent a reactive process to antigenic stimulation. The findings of mixed cellularity in the red pulp composed of monocytes, immunoblasts, and plasma cells are consistent with an infectious process such as that seen in infectious mononucleosis. We did not determine if tissue damage is virally induced or is a byproduct of the host response to infection. One could speculate that much of the damage is complement- and monocyte-driven, as seen in other arthralgic alphaviruses, or perhaps T cell-driven.[45,46] The age-dependent virulence of ONNV is typical of alphaviruses and has been described in numerous rodent models of alphavirus infection and pathogenesis.[28,42,47–55]

Our results also represent progress in developing a murine model to represent human disease after ONNV infection. The STAT1 KO and A129 mice inoculated s.c. do recapitulate the myositis and tenosynovitis that are probably present in humans, as suggested by findings from human infections with the closely related CHIKV. Mice however differ from humans, who are not known to die of ONNV infection.[56] As stated previously, this is in contrast to A129 mice inoculated in the f.p., which show clinical illness, f.p. swelling, and myositis but do not have either neurologic or fatal disease and is most likely closer to human disease than those inoculated by the s.c. route. In addition, STAT1 KO and A129 mice (regardless of route of inoculation) generate a viremia peaking on days 2–3 that wanes by day 5, which is typical of alphavirus infections of humans. The ability to cause neurologic disease appears to be a common property of many alphaviruses.

As seen in earlier studies, 100 pfu of CHIKV is lethal for A129 mice by 3 days post inoculation.[18] This dose is 10-fold lower than the dose of ONNV needed to induce 50% mortality. Mortality increased to 100% when the ONNV dose was increased to 10^4 pfu. These results indicate that ONNV is less virulent than CHIKV in the mouse model. However, it is difficult to say whether ONNV is less virulent than CHIKV in humans. Both of these viruses cause very similar human disease syndromes. Even though fatal ONNV infections have not been described in the literature, surveillance during outbreaks has been less rigorous than during recent CHIKV epidemics. Although mouse models can suggest

differences in pathogenesis, human data from infected individuals are needed to compare the virulence of ONNV and CHIVK in humans.

During this study we used the two available strains of ONNV (SG650 and MP30). These two strains show striking differences in virulence and clinical signs. The SG650 strain is more virulent in the mouse model and caused neurologic signs in only about 10% of STAT1 KO mice inoculated by the s.c. route, whereas it caused no neurologic illness in A129 mice inoculated by the s.c. route. The MP30 strain on the other hand usually caused minimal disease. A dose of 10^4 pfu had to be reached to obtain mortality. However, MP30 caused neurologic signs in all mice that succumbed to illness. Because of the low virulence and propensity to cause neurologic signs when illness does occur, we feel that MP30 infection does not represent a good model of human ONN disease. In contrast, A129 mice inoculated by the f.p. at 10^3 pfu showed clinical illness and f.p. swelling, though no mortality. Therefore, we believe that f.p. inoculation in the A129 mouse most closely resembles human disease. These differences in virulence could be caused by the passage history of the two viral strains. The MP30 strain has been passaged numerous times in suckling mouse brain, whereas SG650 has only been passaged in Vero cells three times. The MP30 strain may be displaying a more neuroadapted phenotype as has been seen in Sindbis virus, which after passage in young mouse brains shows neurotropism and increased neurovirulence.[57]

Although it received little attention for 50 years following its discovery, the recent outbreaks of CHIKV in the Indian Ocean, India, Southeast Asia, and Europe have shown that an arthralgic Old World alphavirus can mutate to cause explosive outbreaks. O'yong-nyong also has the potential to cause large future outbreaks in Africa and possibly elsewhere. Because ONNV uses the same vectors exploited by malaria parasites, *Anopheles* mosquitoes, many locations susceptible to malaria may also be vulnerable to ONNV.

Received November 1, 2012. Accepted for publication January 1, 2013.

Published online April 8, 2013.

Acknowledgments: We thank the Galveston National Laboratory Experimental Pathology Services Division for their assistance with histopathological studies, and Curtis Klages for his veterinary advice.

Financial support: This work was supported by a grant from the National Institute of Allergy and Infectious Disease (NIAID) through the Western Regional Center of Excellence for Biodefense and Emerging Infectious Disease Research, National Institutes of Health (NIH) grant U54 AIO57156, and by NIH grants AI082202 and AI093491. RLS was supported by NIH grant 5T32AI-007536. SLR was supported by NIH grant 5T3AI-007536. KSP was supported by NIH grant 5T327526-12.

Authors' addresses: Robert L. Seymour, Shannan L. Rossi, Nicholas A. Bergren, Kenneth S. Plante, and Scott C. Weaver, Institute for Human Infections and Immunity, Center for Tropical Diseases, and Department of Pathology, University of Texas Medical Branch, Galveston, TX, E-mails: rlseymou@utmb.edu, slrossi@utmb.edu, nabergre@utmb.edu, ksplante@utmb.edu, and sweaver@utmb.edu.

REFERENCES

1. Enserink M, 2006. Infectious diseases. Massive outbreak draws fresh attention to little-known virus. *Science 311:* 1085.
2. Arankalle VA, Shrivastava S, Cherian S, Gunjikar RS, Walimbe AM, Jadhav JM, Sudeep AB, Mishra AC, 2007. Genetic divergence of Chikungunya viruses in India (1963–2006) with special reference to the 2005–2006 explosive epidemic. *J Gen Virol 88:* 1967–1976.
3. Hapuarachchi HC, Bandara KB, Sumanadasa SD, Hapugoda MD, Lai YL, Lee KS, Tan LK, Lin RT, Ng LF, Bucht G, Abeyewickreme W, Ng LC, 2009. Re-emergence of Chikungunya virus in south-east Asia: virological evidence from Sri Lanka and Singapore. *J Gen Virol 91:* 1067–1076.
4. Charrel RN, de Lamballerie X, Raoult D, 2007. Chikungunya outbreaks–the globalization of vectorborne diseases. *N Engl J Med 356:* 769–771.
5. Pialoux G, Gauzere BA, Jaureguiberry S, Strobel M, 2007. Chikungunya, an epidemic arbovirosis. *Lancet Infect Dis 7:* 319–327.
6. Robin S, Ramful D, Le Seach F, Jaffar-Bandjee MC, Rigou G, Alessandri JL, 2008. Neurologic manifestations of pediatric Chikungunya infection. *J Child Neurol 23:* 1028–1035.
7. Haddow AJ, Davies CW, Walker AJ, 1960. O'nyong-nyong fever: an epidemic virus disease in East Africa. 1. Introduction. *Trans R Soc Trop Med Hyg 54:* 517–522.
8. Kiwanuka N, Sanders EJ, Rwaguma EB, Kawamata J, Ssengooba FP, Najjemba R, Were WA, Lamunu M, Bagambisa G, Burkot TR, Dunster L, Lutwama JJ, Martin DA, Cropp CB, Karabatsos N, Lanciotti RS, Tsai TF, Campbell GL, 1999. O'nyong-nyong fever in south-central Uganda, 1996–1997: clinical features and validation of a clinical case definition for surveillance purposes. *Clin Infect Dis 29:* 1243–1250.
9. Sanders EJ, Rwaguma EB, Kawamata J, Kiwanuka N, Lutwama JJ, Sengooba FP, Lamunu M, Najjemba R, Were WA, Bagambisa G, Campbell GL, 1999. O'nyong-nyong fever in south-central Uganda, 1996–1997: description of the epidemic and results of a household-based seroprevalence survey. *J Infect Dis 180:* 1436–1443.
10. Lanciotti RS, Ludwig ML, Rwaguma EB, Lutwama JJ, Kram TM, Karabatsos N, Cropp BC, Miller BR, 1998. Emergence of epidemic O'nyong-nyong fever in Uganda after a 35-year absence: genetic characterization of the virus. *Virology 252:* 258–268.
11. Posey D, O'Rourke T, Roherig JT, Lanciotti RS, Weinberg M, Maloney S, 2005. O'nyong-nyong fever in West Africa. *Am J Trop Med Hyg 73:* 32.
12. Tesh RB, 1982. Arthritides caused by mosquito-borne viruses. *Annu Rev Med 33:* 31–40.
13. Williams MC, Woodall JP, Porterfield JS, 1962. O'nyong-nyong fever: an epidemic virus disease in East Africa. V. Human antibody studies by plaque inhibition and other serological tests. *Trans R Soc Trop Med Hyg 56:* 166–172.
14. Powers AM, Brault AC, Tesh RB, Weaver SC, 2000. Re-emergence of Chikungunya and O'nyong-nyong viruses: evidence for distinct geographical lineages and distant evolutionary relationships. *J Gen Virol 81:* 471–479.
15. Grandadam M, Caro V, Plumet S, Thiberge JM, Souarès Y, Failloux AB, Tolou HJ, Budelot M, Cosserat D, Leparc-Goffart I, Despres P, 2011. Chikungunya virus, southeastern France. *Emerg Infect Dis 17:* 910–913.
16. Johnson BK, Gichogo A, Gitau G, Patel N, Ademba G, Kirui R, Highton RB, Smith DH, 1981. Recovery of O'nyong-nyong virus from *Anopheles funestus* in western Kenya. *Trans R Soc Trop Med Hyg 75:* 239–241.
17. Williams MC, Woodall JP, Corbert PS, Gillett JD, 1965. O'nyong-nyong fever: an epidemic virus disease in East Africa. 8. Virus isolations from *Anopheles* mosquitoes. *Trans R Soc Trop Med Hyg 59:* 300–306.
18. Beaty BJ, Calisher CH, Shope RE, 1989. Arboviruses. Schmidt NJ, Emmons RW, eds. *Diagnostic Procedures for Viral, Rickettsial and Chlamydial Infections*. Sixth edition. Washington, DC: American Public Health Association, 797–855.
19. Plante K, Wang E, Partidos CD, Weger J, Gorchakov R, Tsetsarkin K, Borland EM, Powers AM, Seymour R, Stinchcomb DT, Osorio JE, Frolov I, Weaver SC, 2011. Novel chikungunya vaccine candidate with an IRES-based attenuation and host range alteration mechanism. *PLoS Pathog 7:* e1002142.
20. Partidos CD, Weger J, Brewoo J, Seymour R, Borland EM, Ledermann JP, Powers AM, Weaver SC, Stinchcomb DT, Osorio JE, 2011. Probing the attenuation and protective efficacy of a candidate Chikungunya virus vaccine in mice with compromised interferon (IFN) signaling. *Vaccine 29:* 3067–3073.

21. Smith DR, Carrara AS, Aguilar PV, Weaver SC, 2005. Evaluation of methods to assess transmission potential of Venezuelan equine encephalitis virus by mosquitoes and estimation of mosquito saliva titers. *Am J Trop Med Hyg 73:* 33–39.
22. Labadie K, Larcher T, Joubert C, Mannioui A, Delache B, Brochard P, Guigand L, Dubreil L, Lebon P, Verrier B, de Lamballerie X, Suhrbier A, Cherel Y, Le Grand R, Roques P, 2010. Chikungunya disease in nonhuman primates involves long-term viral persistence in macrophages. *J Clin Invest 120:* 894–906.
23. Herrero LJ, Nelson M, Srikiatkhachorn A, Gu R, Anantapreecha S, Fingerle-Rowson G, Bucala R, Morand E, Santos LL, Mahalingam S, 2011. Critical role for macrophage migration inhibitory factor (MIF) in Ross River virus-induced arthritis and myositis. *Proc Natl Acad Sci USA 108:* 12048–12053.
24. Rulli NE, Rolph MS, Srikiatkhachorn A, Anantapreecha S, Guglielmotti A, Mahalingam S, 2011. Protection from arthritis and myositis in a mouse model of acute Chikungunya virus disease by bindarit, an inhibitor of monocyte chemotactic protein-1 synthesis. *J Infect Dis 204:* 1026–1030.
25. Gunn BM, Morrison TE, Whitmore AC, Blevins LK, Hueston L, Fraser RJ, Herrero LJ, Ramirez R, Smith PN, Mahalingam S, Heise MT, 2012. Mannose binding lectin is required for alphavirus-induced arthritis/myositis. *PLoS Pathog 8:* e1002586.
26. Morrison TE, Simmons JD, Heise MT, 2008. Complement receptor 3 promotes severe Ross River virus-induced disease. *J Virol 82:* 11263–11272.
27. Morrison TE, Fraser RJ, Smith PN, Mahalingam S, Heise MT, 2007. Complement contributes to inflammatory tissue destruction in a mouse model of Ross River virus-induced disease. *J Virol 81:* 5132–5143.
28. Couderc T, Chrétien F, Schilte C, Disson O, Brigitte M, Guivel-Benhassine F, Touret Y, Barau G, Cayet N, Schuffnecker I, Depres P, Arenzana-Seisdedos F, Michault A, Albert ML, Lecuit M, 2008. A mouse model for Chikungunya: young age and inefficient type-I interferon signaling are risk factors for severe disease. *PLoS Pathog 4:* e29.
29. Schilte C, Couderc T, Chretien F, Sourisseau M, Gangneux N, Guivel-Benhassine F, Kraxner A, Tschopp J, Higgs S, Michault A, Arenzana-Seisdedos F, Colonna M, Peduto L, Schwartz O, Lecuit M, Albert ML, 2010. Type I IFN controls Chikungunya virus via its action on nonhematopoietic cells. *J Exp Med 207:* 429–442.
30. Kelvin AA, Banner D, Silvi G, Moro ML, Spataro N, Gaibani P, Cavrini F, Pierro A, Rossini G, Cameron MJ, Bermejo-Martin JF, Paquette SG, Xu L, Danesh A, Farooqui A, Borghetto I, Kelvin DJ, Sambri V, Rubino S, 2011. Inflammatory cytokine expression is associated with Chikungunya virus resolution and symptom severity. *PLoS Negl Trop Dis 5:* e1279.
31. Chaaitanya IK, Muruganandam N, Sundaram SG, Kawalekar O, Sugunan AP, Manimunda SP, Ghosal SR, Muthumani K, Vijayachari P, 2011. Role of proinflammatory cytokines and chemokines in chronic arthropathy in CHIKV infection. *Viral Immunol 24:* 265–271.
32. Chow A, Her Z, Ong EK, Chen JM, Dimatatac F, Kwek DJ, Barkham T, Yang H, Rénia L, Leo YS, Ng LF, 2011. Persistent arthralgia induced by Chikungunya virus infection is associated with interleukin-6 and granulocyte macrophage colony-stimulating factor. *J Infect Dis 203:* 149–157.
33. Nakaya HI, Gardner J, Poo YS, Major L, Pulendran B, Suhrbier A, 2012. Gene profiling of Chikungunya virus arthritis reveals significant overlap with rheumatoid arthritis. *Arthritis Rheum 64:* 3553–3563.
34. Cruz CC, Suthar MS, Montgomery SA, Shabman R, Simmons J, Johnston RE, Morrison TE, Heise MT, 2010. Modulation of type I IFN induction by a virulence determinant within the alphavirus nsP1 protein. *Virology 399:* 1–10.
35. Gardner CL, Yin J, Burke CW, Klimstra WB, Ryman KD, 2009. Type I interferon induction is correlated with attenuation of a South American eastern equine encephalitis virus strain in mice. *Virology 390:* 338–347.
36. Burke CW, Gardner CL, Steffan JJ, Ryman KD, Klimstra WB, 2009. Characteristics of alpha/beta interferon induction after infection of murine fibroblasts with wild-type and mutant alphaviruses. *Virology 395:* 121–132.
37. Simmons JD, White LJ, Morrison TE, Montgomery SA, Whitmore AC, Johnston RE, Heise MT, 2009. Venezuelan equine encephalitis virus disrupts STAT1 signaling by distinct mechanisms independent of host shutoff. *J Virol 83:* 10571–10581.
38. Partidos CD, Paykel J, Weger J, Borland EM, Powers AM, Seymour R, Weaver SC, Stinchomb DT, Osorio JE, 2012. Cross-protective immunity against O'nyong-nyong virus afforded by a novel recombinant Chikungunya vaccine. *Vaccine 30:* 4638–4643.
39. Gardner CL, Burke CW, Higgs ST, Klimstra WB, Ryman KD, 2012. Interferon-alpha/beta deficiency greatly exacerbates arthrogenic disease in min infected with wild-type chikungunya virus but not with the cell culture-adapted live-attenuated 181/25 vaccine candidate. *Virology 425:* 103–112.
40. Morrison TE, Oko L, Montgomery SA, Whitmore AC, Lotstein AR, Gunn BM, Elmore SA, Heise MT, 2011. A mouse model of Chikungunya virus-induced musculoskeletal inflammatory disease: evidence of arthritis, tenosynovitis, myositis, and persistence. *Am J Pathol 178:* 32–40.
41. Gardner J, Anraku I, Le TT, Larcher T, Major L, Roques P, Schroder WA, Higgs S, Suhrbier A, 2010. Chikungunya virus arthritis in adult wild-type mice. *J Virol 84:* 8021–8032.
42. Ziegler SA, Lu L, da Rosa AP, Xiao SY, Tesh RB, 2008. An animal model for studying the pathogenesis of Chikungunya virus infection. *Am J Trop Med Hyg 79:* 133–139.
43. Obeyesekere I, Hermon Y, 1972. Myocarditis and cardiomyopathy after arbovirus infections (dengue and Chikungunya fever). *Br Heart J 34:* 821–827.
44. Obeyesekere I, Hermon Y, 1973. Arbovirus heart disease: myocarditis and cardiomyopathy following dengue and Chikungunya fever–a follow-up study. *Am Heart J 85:* 186–194.
45. Morrison TE, Fraser RJ, Smith PN, Mahalingam S, Heise MT, 2007. Complement contributes to inflammatory tissue destruction in a mouse model of Ross River virus-induced disease. *J Virol 81:* 5132–5143.
46. Rulli NE, Guglielmotti A, Mangano G, Rolph MS, Apicella C, Zaid A, Suhrbier A, Mahalingam S, 2009. Amelioration of alphavirus-induced arthritis and myositis in a mouse model by treatment with bindarit, an inhibitor of monocyte chemotactic proteins. *Arthritis Rheum 60:* 2513–2523.
47. Griffin DE, 1976. Role of the immune response in age-dependent resistance of mice to encephalitis due to Sindbis virus. *J Infect Dis 133:* 456–464.
48. Fleming P, 1977. Age-dependent and strain-related differences of virulence of Semliki Forest virus in mice. *J Gen Virol 37:* 93–105.
49. Jackson AC, Moench TR, Griffin DE, Johnson RT, 1987. The pathogenesis of spinal cord involvement in the encephalomyelitis of mice caused by neuroadapted Sindbis virus infection. *Lab Invest 56:* 418–423.
50. Johnson RT, McFarland HF, Levy SE, 1972. Age-dependent resistance to viral encephalitis: studies of infections due to Sindbis virus in mice. *J Infect Dis 125:* 257–262.
51. Labrada L, Liang XH, Zheng W, Johnston C, Levine B, 2002. Age-dependent resistance to lethal alphavirus encephalitis in mice: analysis of gene expression in the central nervous system and identification of a novel interferon-inducible protective gene, mouse ISG12. *J Virol 76:* 11688–11703.
52. Havert MB, Schofield B, Griffin DE, Irani DN, 2000. Activation of divergent neuronal cell death pathways in different target cell populations during neuroadapted sindbis virus infection of mice. *J Virol 74:* 5352–5356.
53. Nava VE, Rosen A, Veliuona MA, Clem RJ, Levine B, Hardwick JM, 1998. Sindbis virus induces apoptosis through a caspase-dependent, CrmA-sensitive pathway. *J Virol 72:* 452–459.
54. Burdeinick-Kerr R, Griffin DE, 2005. Gamma interferon-dependent, noncytolytic clearance of Sindbis virus infection from neurons *in vitro*. *J Virol 79:* 5374–5385.
55. Griffin DE, 2010. Recovery from viral encephalomyelitis: immune-mediated noncytolytic virus clearance from neurons. *Immunol Res 47:* 123–133.
56. Ozden S, Huerre M, Riviere JP, Coffey LL, Afonso PV, Mouly V, de Monredon J, Roger JC, El Amrani M, Yvin JL, Jaffar MC, Frenkiel MP, Sourisseau M, Schwartz O, Butler-Browne G, Depres P, Gessain A, Ceccaldi PE, 2007. Human muscle satellite cells as targets of Chikungunya virus infection. *PLoS ONE 2:* e527.
57. Lustig S, Jackson AC, Hahn CS, Griffin DE, Strauss EG, Strauss JH, 1988. The molecular basis of Sindbis virus neurovirulence in mice. *J Virol 62:* 2329–2336.